JOURNAL OF GEOPHYSICAL RESEARCH, VOL. 102, NO. B11, PAGES 24,887–24,902, NOVEMBER 10, 1997

Thermal fluxes associated with the 1993 diking event on the CoAxial segment, Juan de Fuca Ridge: A model for the convective cooling of a dike

Abdellah S. M. Cherkaoui and William S. D. Wilcock

School of Oceanography, University of Washington, Seattle

Edward T. Baker

Pacific Marine Environmental Laboratory, NOAA, Seattle, Washington

Abstract. The 1993 diking event on the CoAxial segment, northern Juan de Fuca Ridge, generated at least three hydrothermal event plumes high in the water column and lower chronic plumes along ~40 km of the ridge axis. A 2-year time series of temperature and light attenuation measurements within the water column shows a rapid decay of the maximum rise height of the chronic plumes over the first 3 months following the eruption. We use these measurements to estimate the hydrothermal heat fluxes into the chronic plumes at two different sites. We hypothesize that the chronic plumes resulted from the convective cooling of a dike and construct a simple two-dimensional, numerical model of this process for a vertical dike intruded into a cold, saturated porous layer. The width of the dike and the permeability and thickness of the porous layer control the transfer of heat from the dike to the seafloor. We investigate the effects of these parameters on the temporal evolution of the surficial heat fluxes. The results show that simple convective cooling of the dike can reproduce the observed temporal evolution of the heat fluxes for permeabilities in the range 10^{-11}-10^{-12} m^2 and a 3- to 5-m-wide dike. The high permeabilities obtained are consistent with flow through highly permeable extrusives or with the creation of a zone of high permeability near the dike walls due to fracturing. The width of the dike may well be overestimated by our model because of the limitations of the continuum approximation for the permeability in the narrow upflow zone adjacent to the dike.

1. Introduction

Mid-ocean ridge volcanism and plutonism account for about 70% of the Earth's magmatic budget [*Crisp*, 1984]. Magma is fed to the upper oceanic crust through vertical dikes oriented parallel to the ridge axis. The thick layers of sheeted dikes and extrusive basalts observed in ophiolites [e.g., *Kidd*, 1977] and in oceanic crustal sections [e.g., *Francheteau et al.*, 1992] attest to the importance of this process in the formation of oceanic crust. Diking events not only control the episodic transport of magma to the surface but also dramatically affect hydrothermal discharge [*Haymon et al.*, 1993; *Embley and Chadwick*, 1994]. On a geological timescale, diking events are instantaneous and very frequent, making repeated observations possible in the human time frame. Before the U.S. Navy's Sound Surveillance System (SOSUS) hydrophone arrays became available to monitor seafloor seismicity [*Fox*, 1995], such events were difficult to detect because diking-related earthquakes have magnitudes below the threshold of teleseismic arrays. Observations of seafloor diking events are still very sparse.

To date, evidence for very recent eruptions has been found on the Cleft and CoAxial segments of the Juan de Fuca Ridge [*Chadwick and Embley*, 1994; *Fox*, 1995], on the East Pacific Rise (EPR) [*Renard et al.*, 1985; *Macdonald et al.*, 1989; *Haymon et al.*, 1993], and most recently on the northern Gorda Ridge [*Baker et al.*, 1996]. On the southern East Pacific Rise, new lava flows were observed from a submersible [*Renard et al.*, 1985] or were inferred from SeaMarc II records [*Macdonald et al.*, 1989]. On the Cleft segment, indirect evidence came from the discovery of large bodies of anomalously warm seawater associated with the catastrophic release of hydrothermal fluids high in the water column in 1986 and 1987 [*Baker et al.*, 1987, 1989]. *Baker et al.* [1987] hypothesized that these ephemeral event plumes were diking related. Subsequent bathymetric studies and underwater observations provided strong support for this suggestion [*Embley et al.*, 1991; *Chadwick et al.*, 1991]. Direct observations of an eruptive diking event on the seafloor were first reported by *Haymon et al.* [1993], who fortuitously came across a very recent eruption while diving above the axial summit caldera on the EPR at 9°50'N.

The CoAxial event of June 1993 is the first diking event to be detected remotely and monitored by the SOSUS hydrophone arrays [*Fox*, 1995]; it is also the first submarine diking event for which seafloor observations are correlated with measurements in the hydrothermal plumes [*Baker et al.*, 1995a] and with seismic data which constrain the temporal and spatial characteristics of dike emplacement [*Fox et al.*, 1995; *Dziak et al.*, 1995]. During the 2 years following the eruption, several oceanographic cruises visited the site [*Baker et al.*, 1993; *De-*

Paper number 97JB02123.
0148-0227/97/97JB-02123$09.00

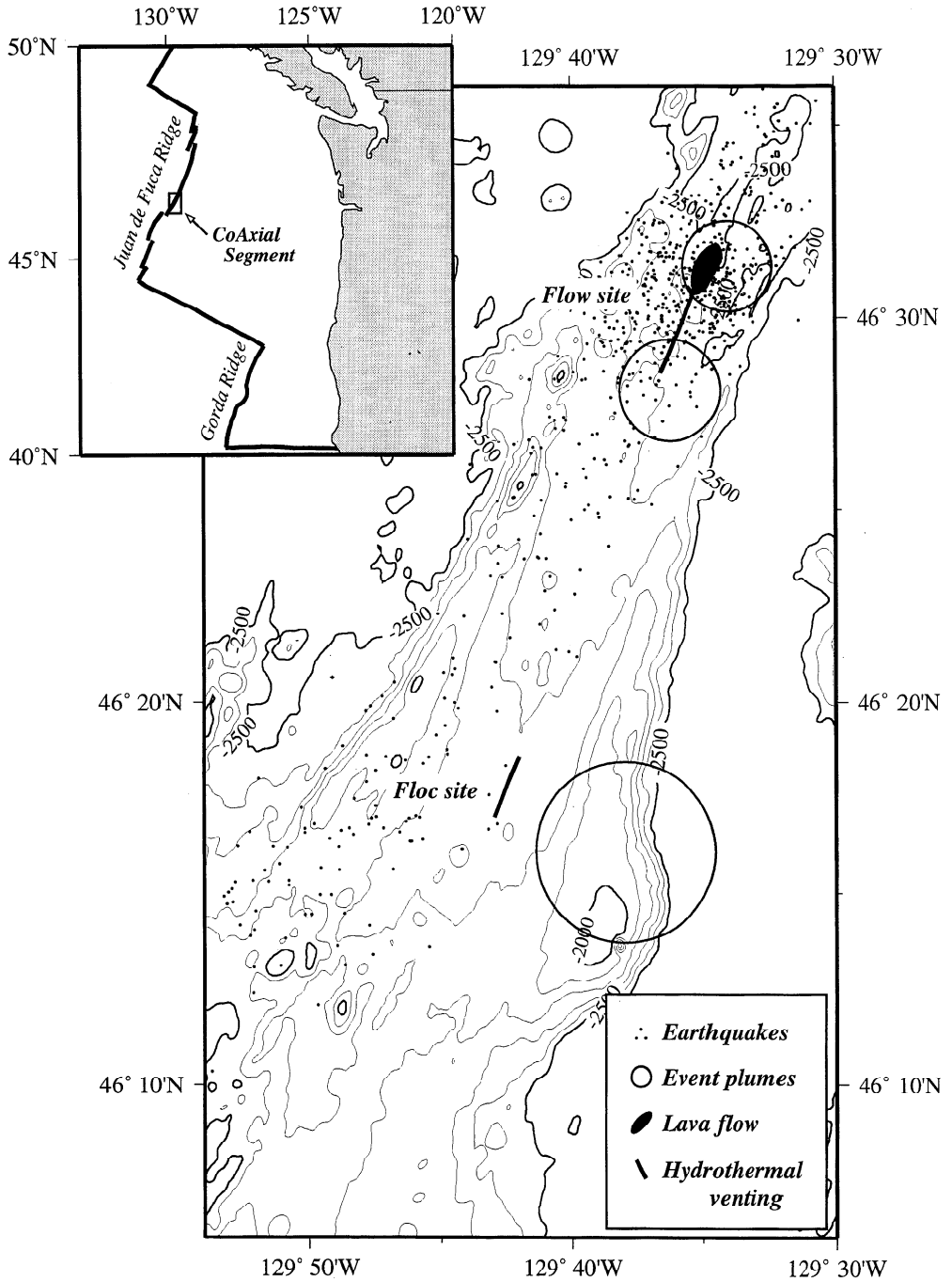

Figure 1. SeaBeam bathymetric map of the CoAxial segment, Juan de Fuca Ridge (100-m contours). The solid dots show the epicenters of the earthquakes detected by the U.S. Navy Sound Surveillance System (SOSUS) hydrophone arrays [*Dziak et al.*, 1995]. The seismicity started to the south on June 23, 1993, and propagated downslope to the north over 2 days to ~46°32'N where earthquake swarms continued for 2 weeks. The solid area shows the limits of the new lava flow discovered in July 1993 [*Embley et al.*, 1995]. Bold lines mark the extent of the hydrothermal venting observed in July 1993 with the remotely operated vehicle ROPOS [*Embley et al.*, 1995], and open circles show the locations and extent of the three event plumes found high in the water column during the same period [*Baker et al.*, 1995a].

laney and Embley, 1993; *Spiess and Hildebrand*, 1993; *Embley et al.*, 1994], yielding an extensive time series of seafloor and water column observations. The CoAxial diking event provides a unique data set that can constrain how dikes cool and how they perturb the flow of hydrothermal fluids. In this study we hypothesize that the heat fluxes carried by the chronic plumes result from the cooling of the dike. We use the 2-year time series of water column measurements above the CoAxial segment to estimate the decay of the heat fluxes following the diking event. We combine these data with a numerical model of the convective cooling of a molten dike to constrain the physical parameters controlling the transfer of

heat from the dike to the seafloor. These parameters are the bulk permeability, the dike width, and the thickness of the permeable layer intruded by the dike.

2. The CoAxial Event

The CoAxial segment is an 80-km-long linear rift on the Juan de Fuca Ridge (Figure 1). It extends northward of Axial volcano, and deepens from ~2100 to ~2500 m below sea level at its northern end. It is offset to the south by the northern rift of Axial volcano and to the north by the Cobb segment. Beginning June 26, 1993, earthquake-generated tertiary waves were recorded by the U.S. Navy SOSUS hydrophone arrays [*Fox*, 1995]; the seismicity indicated that the swarm started at the southern end of the CoAxial segment near 46°15'N and migrated over 2 days to the north, downslope along the axial ridge, to ~46°36'N where the earthquakes continued for 2 weeks. The patterns of the seismicity are suggestive of a lateral dike injection with eruptive volcanism [*Dziak et al.*, 1995]. Seafloor observations during July 1993 [*Embley et al.*, 1995] revealed a fresh lava flow at the northern end of the seismicity, centered around 46°32'N (the flow site). The new flow extended 2.5 km along axis and was up to 300 m wide. Warm water was venting almost continuously along the axis of the fresh, unfractured lava flow and from fractures within a 20- to 40-m-wide graben extending at least 4 km south of the new eruption. Hydrothermal venting was also observed near 46°19'N (the floc site), where an intense near-bottom thermal signal in the water column [*Embley et al.*, 1995] was accompanied by a cloud of white, flocular, bacterial material [*Juniper et al.*, 1995]. These early bottom observations were limited to the flow and the floc sites. Water column surveys conducted prior to 1993 showed no evidence of hydrothermal discharge from the flow and the floc sites [*Baker et al.*, 1997].

Along with the seafloor observations, extensive water column measurements were obtained during the initial field response [*Embley et al.*, 1995; *Baker et al.*, 1995a]. Temperature and light attenuation anomalies were mapped along the segment axis using a conductivity-temperature-depth (CTD) and transmissometer package which was cycled vertically while being towed through the water. These measurements revealed the presence of two kinds of plumes (Figure 2). A lower chronic plume, rising about 400 m above the seafloor, extended ~40 km from 46°14'N to 46°34'N. Two well-defined event plumes, rising nearly 1000 m above the seafloor, were present directly above the lava intrusion [*Baker et al.*, 1995a]. A third event plume was located 2 weeks later, 30 km south of the lava flow (Figure 1). Unlike the chronic plumes, the three event plumes were short-lived and were advected away in less than 2 weeks [*Cannon et al.*, 1995]. Subsequent cruises to the event site in August, September, and October 1993, and in the summers of 1994 and 1995 [*Baker et al.*, 1993; *Delaney and Embley*, 1993; *Embley et al.*, 1994; *Butterfield et al.*, 1997] yielded additional seafloor observations and water column measurements within the chronic plumes. Table 1 presents the time series of the maximum observed rise heights of the chronic plumes above the flow and the floc sites; the rise heights decreased rapidly over the first 3 months. One year after the diking event, submersible observations showed that seafloor venting had almost ceased at the flow site and had diminished considerably at the floc site [*Embley et al.*, 1994; *Butterfield et al.*, 1997]. In the following section we use the rise heights of the chronic plumes to estimate the heat fluxes.

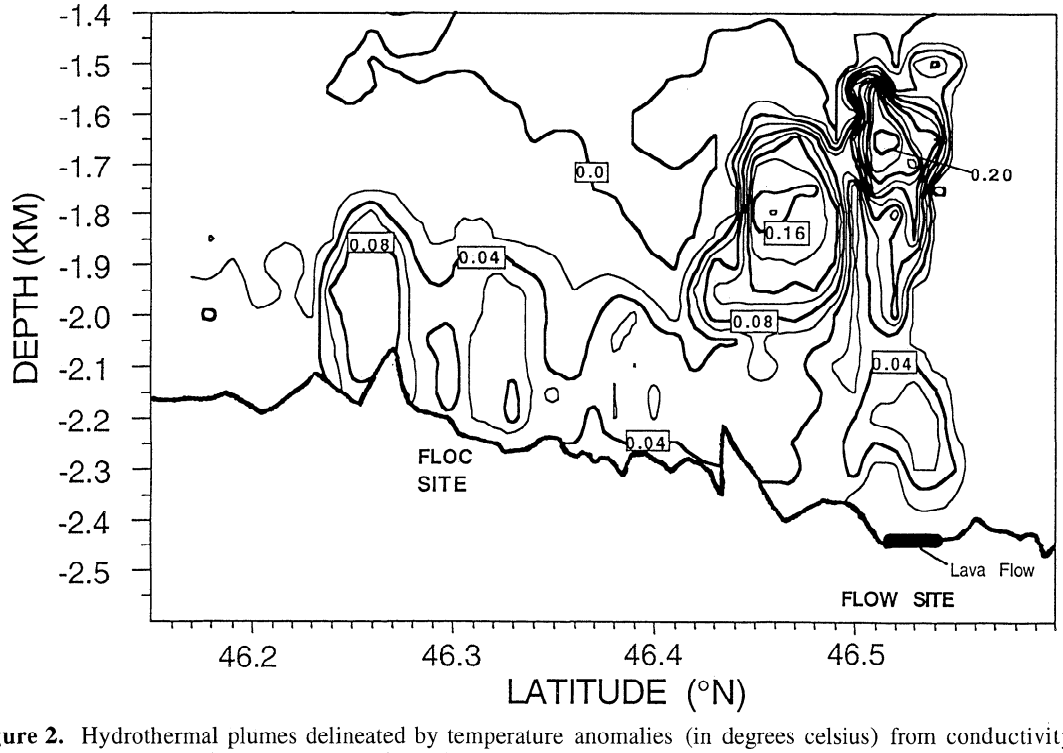

Figure 2. Hydrothermal plumes delineated by temperature anomalies (in degrees celsius) from conductivity-temperature-depth (CTD) measurements along the axis of the CoAxial segment (0.02°C contour interval). The plumes were mapped on July 11, about 2 weeks after the onset of the seismicity. Chronic plumes were nearly continuous from 46°15' to 46°33'N, with a typical rise height of ~400 m at this time. Two event plumes above the flow site have rise heights of nearly 1000 m.

Estimation of the Heat Fluxes

Hydrothermal fluids rise in the water column because of the combined effect of thermal and chemical buoyancy. The chemical compositions of the fluids that vented at the flow and floc sites following the diking event [*Butterfield et al.*, 1997] are such that the buoyancy attributable to salinity deficits is negligible compared to that induced by temperature excesses. The maximum rise height of an ideal thermal plume emanating from a point source [*Morton et al.*, 1956; *Turner*, 1973] is dependent upon its initial buoyancy flux B_0

$$B_0 = \frac{\alpha g Q_H}{\rho_0 c_{p_f}} \tag{1}$$

and the ambient buoyancy frequency N, a function of the regional density gradient in which the plume rises

$$N = \left(\frac{g}{\rho_0} \frac{\partial \rho}{\partial z} \right)^{\frac{1}{2}} \tag{2}$$

where Q_H is the rate of discharge of heat at the source, ρ_0 is a reference density (average local density), α is the coefficient of thermal expansion, c_{pf} is the specific heat capacity, and g is the acceleration of gravity. Dimensional analysis [*Morton et al.*, 1956; *Turner*, 1973] shows the quantity $B_0^{1/4}N^{-3/4}$ has units of length. Experimental observations of buoyant plumes from a point source in continuously stratified environments [*Briggs*, 1969; *Turner*, 1986] show that over a wide range of values of B_0 and N the maximum rise height is

$$z_{\max} = 5\left(\frac{B_0}{\pi} \right)^{1/4} N^{-3/4} \tag{3}$$

For a plume emanating from a line source of length l the buoyancy flux is

$$B_0 = \frac{\alpha g Q_H}{\rho_0 c_{p_f} l} \tag{4}$$

and the quantity $B_0^{1/3}N^{-1}$ has units of length. The empirical relation determined for point source plumes (equation (3)) suggests that line sources exhibit a similar invariance, and we assume that the maximum rise height can be expressed

$$z_{\max} = \tilde{z}_{\max} B_0^{1/3} N^{-1} \tag{5}$$

where $\tilde{z}_{\max}$ is a constant dimensionless maximum rise height. This assumption is supported by the work of *Lavelle* [1995], who modeled numerically the rise of the CoAxial event plumes from a line source and found that $\tilde{z}_{\max} \approx 3.7$, a value which is very similar to the constant $5\pi^{-1/4}$ (3.75) used for point-source plumes.

Although the precise pattern of venting is not very well known, we believe the CoAxial chronic plumes are best modeled by a line source. The water column observations (Figure 2) show that soon after the eruption, chronic plumes extended almost continuously from ~46°14'N to ~46°34'N. The initial seafloor observations were limited to the new lava flow area [*Embley et al.*, 1995] and revealed extensive venting along the 2.5-km-long lava flow and along linear fractures within the 4-km-long graben just south of it. Seafloor observations were not made at the floc site until October 1993 [*Butterfield et al.*, 1997], but at this time, there were still many sources along a 4-km-long section of the ridge (D. A. Butterfield, personal communication, 1996). These results do not prove that venting was continuous along axis at the seafloor, but a linear set of closely spaced vents will have essentially the same effect as a continuous linear source. The assumption of a line source for the chronic plumes also requires that the length of the source and the rise height of the plume be much larger than the width of the source. Water column observations suggest this was true for at least several months following the diking event.

Estimates of heat fluxes obtained from the maximum rise height of hydrothermal plumes are associated with considerable uncertainties [*Lupton*, 1995; *McDuff*, 1995]. The rise height is very sensitive to the buoyancy frequency (equation (5)), and it can be difficult to determine the appropriate ambient buoyancy frequency for deep-sea hydrothermal plumes. Because the CoAxial chronic plumes rise in waters already contaminated by hydrothermal fluids, it is inappropriate to take the buoyancy frequency of the background waters far from the plumes. In Figure 3 we compare the decay of the heat fluxes of the chronic plumes at the flow site obtained using the two different sets of buoyancy frequencies which are listed in Table 1. N_{out} is the neighboring buoyancy frequency measured just outside the plumes and is different from the buoyancy frequency well away from the plumes. N_{in} was measured directly in the plumes. N_{out} and N_{in} might be considered upper and lower bounds for the appropriate buoyancy frequency. Figure 3 shows that the choice of the buoyancy frequency has little effect on the overall rate of decay of the heat fluxes, but the absolute value of the heat fluxes differs on average by a factor of about 5 (Table 1). We choose to use N_{out} because these values are more uniform and produce less scatter in the heat flux estimates.

In addition to the uncertainties resulting from the choice of buoyancy frequency, there are two additional sources of systematic error, both of which may bias heat flux estimates to

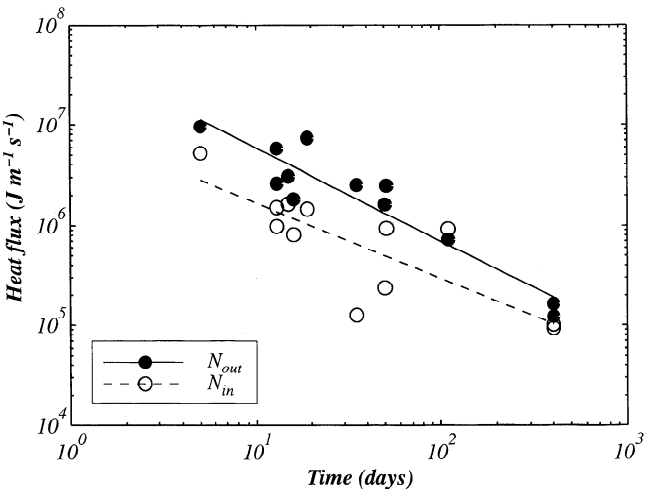

Figure 3. Heat fluxes per unit meter of source at the flow site estimated from the maximum rise heights of the chronic plumes assuming a line source model (see text). We compare the heat fluxes obtained with the two different buoyancy frequencies given in Table 1. The ambient buoyancy frequency (N_{out}, solid circles) is determined just outside the hydrothermal plumes. The plume buoyancy frequency (N_{in}, open circles) is determined within the neutrally buoyant plumes. Straight lines show the logarithmic least squares fit to the estimated heat fluxes. Although there are significant differences in the absolute value of the heat fluxes, the choice of the buoyancy frequency has little effect on the estimated decay time of the heat fluxes.

Table 1. Time Series of Rise Heights and Buoyancy Frequency Observations for the Chronic Hydrothermal Plumes Following the 1993 CoAxial Diking Event

	Time,[1] days	z^*,[2] m	N_{out},[3] s^{-1} x 10^3	Q_{out},[4] MW m^{-1}	N_{in},[5] s^{-1} x 10^3	Q_{in},[6] MW m^{-1}
Flow Site	5	555	1.00	9.57	0.81	5.23
	13	470	1.00	5.81	0.64	1.52
	13	360	1.00	2.61	0.72	0.98
	15	380	1.00	3.07	0.81	1.65
	16	320	1.00	1.83	0.76	0.81
	19	450	1.13	7.38	0.66	1.47
	35	300	1.18	2.54	0.44	0.13
	50	295	1.04	1.63	0.55	0.24
	51	340	1.04	2.49	0.75	0.94
	110	260	0.90	0.72	0.98	0.93
	402	160	0.89	0.16	0.76	0.10
	403	145	0.89	0.12	0.81	0.09
Floc Site	5	450	1.18	8.57	0.61	1.16
	13	480	1.18	10.40	0.61	1.39
	13	380	1.18	5.16	0.50	0.39
	19	440	1.18	8.01	0.73	1.87
	35	460	1.18	9.16	1.02	5.93
	50	450	1.04	5.78	0.68	1.59
	105	330	0.90	1.48	0.24	0.03
	107	340	0.90	1.62	0.29	0.05
	402	230	0.89	0.49	0.53	0.10
	403	230	0.89	0.49	0.38	0.04

[1] Relative to June 29, 1993, the onset time of seismicity at the flow site.

[2] Maximum rise height of the hydrothermal plumes deduced from the temperature anomalies. Note that z^* is likely to be slightly underestimated because the plane of the CTD measurements does not always coincide with the true maximum rise height of the plume.

[3] Buoyancy frequency measured just outside the hydrothermal plumes.

[4] Heat flux per unit meter of source length calculated using N_{out} in (4) and (5) with g = 9.8 m s^{-2}, $\rho_0 c_p$ = 4.0 x 10^6 J m^{-3} °C^{-1}, α = 1.3 x 10^{-4} °C^{-1}.

[5] Buoyancy frequency measured within the hydrothermal plumes.

[6] Same as Q_{out} but using N_{in}.

low values [*Lupton,* 1995; *McDuff,* 1995]. First, each estimate of z_{max} was obtained from CTD measurements on a single vertical plane [*Baker et al.,* 1995b] which may not have crossed the plumes at their maximum height. Second, bottom currents bend the plumes and decrease z_{max} [*Middleton and Thomson,* 1986]. Variable bottom currents with maximum speeds of 14-20 cm s^{-1} were recorded at CoAxial between August 1993 and April 1994 [*Cannon et al.,* 1995].

Figure 4 shows the heat flux estimates obtained from (5) using N_{out}. Although there is considerable scatter in the individual measurements, the heat fluxes show a very clear trend. Both time series decay rapidly, reaching 20% of their maximum value within about 50 days at the flow site and about 90 days at the floc site. These decay times are not sensitive to the choice of buoyancy frequency or to our assumption that the plumes formed from a line source rather than a point source. However, the absolute heat fluxes are sensitive to these potential sources of error, and so we make the conservative assumption that they are associated with an uncertainty of an order of magnitude. In the following sections we investigate whether convective hydrothermal cooling of a vertical dike can reproduce the decay times of the heat fluxes and match the weaker constraints on the absolute heat flux.

4. Numerical Model

Several studies have investigated steady and transient porous convection along an isothermal vertical flat plate [*Cheng and Minkowycz,* 1977; *Parmentier,* 1979; *Cheng and Pop,* 1984; *Delaney,* 1987] but did not include the effects of the finite heat content of a dike. *Patterson and Lowell* [1982] and *Brikowski and Norton* [1989] have studied the problem of

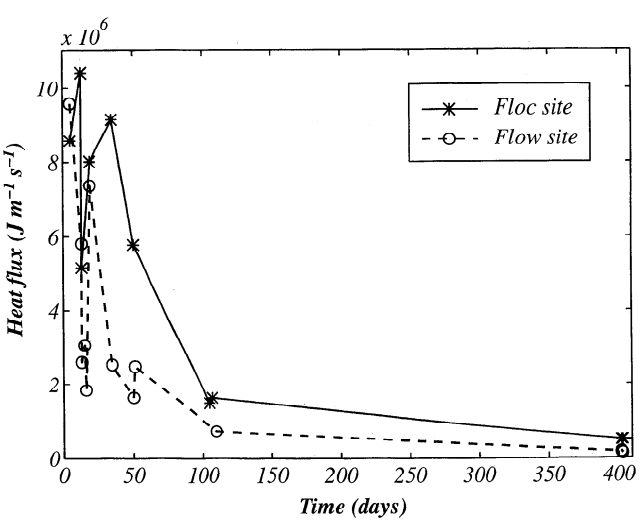

Figure 4. Estimated heat fluxes per unit meter of source using the buoyancy frequency determined just outside the plumes. Time is plotted relative to June 29, 1993, the onset of the seismicity at the flow site [*Dziak et al.,* 1995]. The scatter in the data is probably due to the difficulties associated with estimating the heat fluxes from rise height measurements (see text). Despite the scatter the heat flux data show a clear decline on a time scale of 1-3 months.

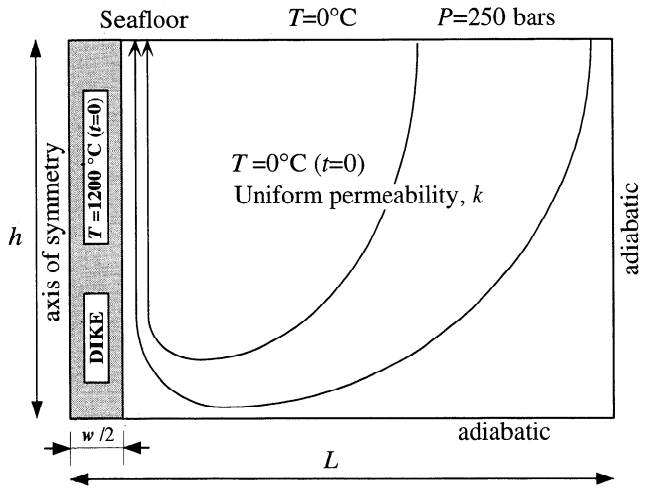

Figure 5. Schematic diagram of the numerical model used in this study. A molten dike, of width w, is injected at a temperature of 1200°C into a cold, fluid-saturated, porous layer of uniform permeability k and thickness h. The dike is impermeable at all times, and the latent heat of magma solidification is included in the calculations. The top boundary is permeable and isothermal; the left boundary is an axis of symmetry; and the right and bottom boundaries are impermeable and adiabatic.

convective cooling above and to the sides of a large magmatic intrusion. Here we consider a simple two-dimensional model of hydrothermal circulation following the intrusion of a thin dike (Figure 5). A vertical, tabular dike is injected at time zero into a fluid-saturated porous layer of thickness h, uniform permeability k, and initial temperature 0°C. The molten dike, of full width w, is injected at an initial temperature of 1200°C, and the latent heat of magma solidification is considered. The dike is impermeable at all times. The top boundary (seafloor) is isothermal (0°C), isobaric (250 bars), and permeable; the left boundary is a mirror plane; and the other two boundaries are adiabatic and impermeable. The width L of the model is chosen large enough so that the flow pattern near the dike is unaffected by the right boundary. Unless otherwise specified all results were obtained with an aspect ratio $h/L = 1$.

We limited our model to the case of single-phase incompressible Darcy flow in a porous medium with uniform rock properties and temperature-dependent fluid properties. Under the Boussinesq approximation the governing equations are [*Bear*, 1972]

$$\nabla \cdot \mathbf{V} = 0 \tag{6}$$

$$\mathbf{V} = \frac{k}{\mu}(-\nabla P + \rho \mathbf{g}) \tag{7}$$

$$(\rho_0 c_p)_m \frac{\partial T}{\partial t} + (\rho_0 c_p)_f \mathbf{V} \cdot \nabla T = \lambda_m \nabla^2 T \tag{8}$$

where $\mathbf{V}$ is the Darcy velocity of the fluid (i.e., a volume flux across a unit area), ∇P is the net pressure gradient, T is the temperature, ρ is the density of the fluid, ρ_0 is the reference density for the Boussinesq approximation (density of the cold fluid), μ is the dynamic viscosity of the fluid, $(\rho_0 c_p)_f$ denotes the heat capacity per unit volume of the fluid, α is the coefficient of thermal expansion for the fluid, and $(\rho_0 c_p)_m$ and λ_m are the heat capacity per unit volume and thermal conductivity of the fluid-saturated rock, respectively.

Because the temperature changes following the dike injection are large, nonlinear fluid properties have a significant effect on the heat fluxes. Measurements of the viscosity of aqueous solutions of sodium chloride in the range 0-350°C at 200 bars [*Yusufova et al.*, 1978] show that the viscosity of seawater differs from that of pure water by only a small factor. We approximate the dynamic viscosity of seawater in the range 0-1200°C using properties for pure water at 250 bars [*Grigull*, 1984], corrected by a constant factor of 0.9 which is the ratio of the viscosity of pure water to seawater at 10°C and 1 bar [*Pond and Pickard*, 1983]. We approximate the temperature-dependent density of seawater by that of a 3.2 wt % solution of NaCl at 250 bars [*Pitzer et al.*, 1984; *Anderko and Pitzer*, 1993]. Above the two-phase boundary we use the properties of the volumetrically dominant phase. We assume a constant heat capacity per unit volume $(\rho c_p)_f = 4.16 \times 10^6$ J m^{-3} °K^{-1} (cold water at 250 bars). For the rock properties we used $\lambda_m = 2$ W m^{-1} °K^{-1}, $(\rho c_p)_m = 3.36 \times 10^6$ J m^{-3} °K^{-1}, and a latent heat of 320 kJ kg^{-1} [*Touloukian et al.*, 1981]. In our Boussinesq formulation variations in fluid density are only accounted for in the buoyancy term of (7). *Gartling and Hickox* [1985] have shown that integrated heat transfer quantities are relatively insensitive to the Boussinesq approximation which can be used over a temperature range of several hundred degrees with only minor inaccuracies. We neglect phase change effects because they are limited to the first few days following the dike emplacement [*Xu and Lowell*, 1996], whereas the decay times we seek to model are of the order of months.

Equations (6)-(8) were nondimensionalized and solved numerically using a finite-volume formulation [*Patankar*, 1980]. We benchmarked our numerical code against the analytical solution for the solidification of a dike by conduction [*Turcotte and Schubert*, 1982] and against previously published numerical solutions for steady convection in a porous layer heated from the side [*Walker and Homsy*, 1978; *Shiralkar et al.*, 1983; *Ni and Beckermann*, 1991]. Both benchmarks show excellent agreement (Tables 2a and 2b). We performed thorough numerical experiments and used grid refinement techniques to establish the optimal spatial and temporal resolution. To resolve the temperature and fluid velocity gradients which are

Table 2a. Benchmark 1: One-Dimensional Conductive Solidification of a Dike

	This Paper	Analytical solution [1]
Time to solidify the dike, days	10.85	10.86
Temperature at the dike boundary, °C	588.7	589

Based on a 2-m-wide intrusion of magma at 1000°C with a thermal diffusivity of 5×10^{-7} m^2 s^{-1}, a specific heat of 1.2 kJ kg^{-1} K^{-1}, and a latent heat of magma solidification of 320 kJ kg^{-1}.

[1] From *Turcotte and Schubert* [1982].

Table 2b. Benchmark 2: Two-Dimensional Convection in a Porous Box Heated From the Side

	Rayleigh Number	This Paper	*Ni and Beckermann* [1991]	*Shiralkar et al.* [1983]	*Walker and Homsy* [1978]
Nusselt number	100	3.102	3.103	3.115	3.097
	500	8.880	8.892	8.944	8.66
	1000	13.27	13.42	13.534	12.96

Steady state solution of natural convection in a two-dimensional, closed, square box filled with a porous medium of uniform permeability. The horizontal and vertical boundaries are adiabatic and isothermal, respectively. The dimensionless Rayleigh number characterizes the vigor of convection within the box and the Nusselt number represents the efficiency of heat transport across the box [*Turcotte and Schubert*, 1982]. Our numerical solution is based on a 50 x 50 uniform grid.

initially very high near the dike boundary, we used nonuniform discretizations both in space and time. All the numerical solutions presented in this paper were obtained with a mesh of 100 x 60 control volumes. The mesh is uniform in the vertical direction. In the horizontal direction, 20 control volumes are spaced evenly across the dike, while outside the dike the spacing increases away from the dike according to the power law

$$dx_i = L \cdot \left(\frac{i}{n}\right)^p \tag{9}$$

where dx_i is the width of the ith of n cells in the horizontal direction. A power $p = 2.2$ allows sufficient resolution at the dike boundary. All the simulations cover 400 days with the same power law (equation (9)) for the time stepping. We used 90 time steps and an initial time step of 1 hour for all the simulations except for $k > 10^{-11}$ m^2, for which we used up to 700 time steps and an initial time as small as 100 s. Above $k = 10^{-10}$ m^2, accurate solutions are computationally too expensive to be included in this study.

The thermal flux Q_H in the country rock across a horizontal boundary at depth Z can be obtained from a solution to (6)-(8) by integrating the conductive and advective heat fluxes across that boundary:

$$Q_H = \int_{w/2}^{L} \left(\left(\rho c_p\right)_f vT - \lambda_m \frac{\partial T}{\partial z} \right)_{z=Z} dx \tag{10}$$

where v is the vertical component of the Darcy velocity. We wish to estimate heat fluxes at the seafloor. At $z = 0$ the top boundary condition $T = 0$ ensures that the advective fluxes are zero (in our continuum model the heat advected from depth is conducted across a very thin surface thermal boundary layer). However, because of the staggered nature of the finite volume grid [*Patankar*, 1980], we estimate the seafloor heat fluxes at a depth corresponding to the center of the uppermost row of control volumes.

5. Numerical Solutions

The transfer of heat from the dike to the seafloor is controlled by the interplay between horizontal conduction across the dike wall and vertical advection within the porous layer. Initially, the heat transfer is dominated by conduction because high horizontal temperature gradients exist across the dike wall. As time progresses, the heat transfer characteristics change from transient one-dimensional heat conduction to two-dimensional free convection. Figure 6 illustrates the flow and the temperature distribution 10 days after the injection of a 2-m-wide dike in a 500-m-thick porous layer with $k = 10^{-12}$ m^2. The convective cell forms a single-pass flow with very well defined regions of upflow and downflow. The pressures are close to cold hydrostatic and upflow is confined to a narrow vertical strip, a few meters wide, adjacent to the dike.

In contrast to earlier steady-state solutions for vertical convection driven by a vertical isothermal plate [*Cheng and Minkowycz*, 1977; *Parmentier*, 1979; *Cheng and Pop*, 1984] the heat input by the dike is finite. The surficial heat flux Q_H rapidly reaches a maximum value and then gradually decays. For a given dike width and layer thickness the temporal evolution of Q_H is controlled by the permeability. Figure 7 shows the maximum temperature T_{max} as a function of the distance x from a 2-m-wide dike for four permeabilities in the range 10^{-10}-10^{-13} m^2. At high permeabilities the rate of heat transport by vertical advection greatly exceeds horizontal conduction. Vertical advection limits the thermal effects of the dike to a region extending only a few meters from the dike. As the permeability decreases, vertical flow velocities also decrease, so that horizontal conduction controls the temperature structure in the porous layer for a longer period of time and further away from

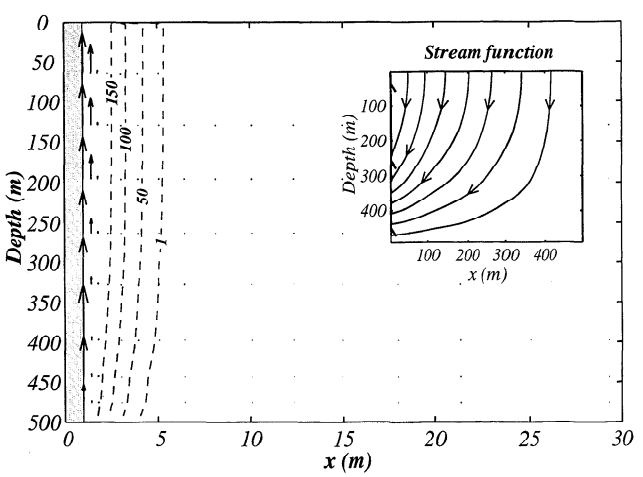

Figure 6. Model configuration 10 days after the intrusion for a simulation with a dike of full width $w = 2$ m, injected into a fluid-saturated porous layer of uniform permeability $k = 10^{-12}$ m^2 and a thickness $h = 500$ m. The dashed lines are temperature contours (150, 50, 10, and 1°C) and the arrows show the direction and relative intensity of the flow. In the example shown, the maximum Darcy velocity is ~10^{-4} m s^{-1}. Note that the main figure only shows the 30 m adjacent to the dike because the thermal effects of the diking intrusion and the upwelling limb of the convective cell are confined to a narrow zone adjacent to the dike. The inset figure shows the streamlines for downflow over the entire computational domain.

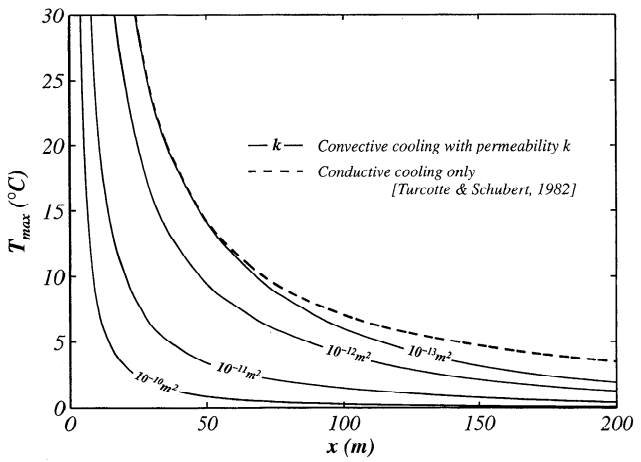

Figure 7. Maximum observed temperature as a function of distance x from the dike. Solid lines are derived from monitoring temperature at 250 m depth in numerical simulations for a 2-m-wide dike intruded into a 500-m-thick layer with permeabilities in the range 10^{-10}-10^{-13} m^2. The dashed line shows an analytical solution for the conductive cooling of the dike [*Turcotte and Schubert,* 1982]. At high permeabilities, vertical advection limits the thermal effects of the dike to a narrow region, a few meters wide, adjacent to the dike. As the permeability decreases, conduction transfers heat further out into the host rock.

the dike. As the permeability approaches zero, the temperature field is that for purely conductive cooling. The dashed line shows an analytical solution for conductive cooling [*Turcotte and Schubert,* 1982, equation (4-163)]. This solution is obtained assuming a planar heat source and is valid at distances that are large compared to the width of the dike.

Figure 8 presents seafloor heat fluxes from simulations performed with a 2-m-wide dike, a 500-m-thick layer, and permeabilities ranging from 10^{-10} to 10^{-15} m^2. Figure 8a shows the maximum heat fluxes, while Figure 8b shows the temporal evolution of these heat fluxes normalized to their maxima. Above $k = 10^{-13}$ m^2 the seafloor heat fluxes are predominantly advective, the maximum value of the advected heat fluxes increases linearly with permeability (Figure 8a), and the time required for Q_H to reach its maximum decreases with permeability (Figure 8b). Below $k = 10^{-13}$ m^2 the normalized curves are identical for longer periods of time. At these lower permeabilities, advection has a negligible effect, and the temperature structure of the porous layer is controlled by horizontal conduction. For permeabilities below 10^{-14} m^2 the maximum thermal flux is nearly constant (Figure 8a) and corresponds to the maximum conductive heat flux at the top of our model.

For a given permeability the temporal evolution of the surficial heat fluxes is controlled by the width of the dike and the thickness of the porous layer. The width of the dike affects the total heat input in the porous layer whereas the layer thickness affects both the total heat and the vertical extent of advection. Figure 9 shows the effect of these two parameters on the surficial heat fluxes for a fixed permeability of 10^{-12} m^2. In Figure 9a the solutions are obtained for six different dike widths ranging from 1 to 6 m and a layer thickness of 500 m. Any two curves coincide as long as the thinnest dike has not completely solidified because the heat flux across the dike wall is independent of the dike width during solidification [*Turcotte and Schubert,* 1982]. The maximum heat flux increases with dike width up to about 4 m, then remains constant at ~9×10^5 J m^{-1} s^{-1}. For wider dikes the maximum heat flux is limited by the maximum rate of advection which depends only upon the permeability. Figure 9b shows solutions obtained for a layer thickness in the range 100-2000 m with a dike width of 2 m and a permeability of 10^{-12} m^2. The maximum value of the heat fluxes increases with thicknesses up to $h \approx 600$ m then remains constant. As for dike width, this maximum value of the heat flux is controlled by the maximum rate of advection. The in-

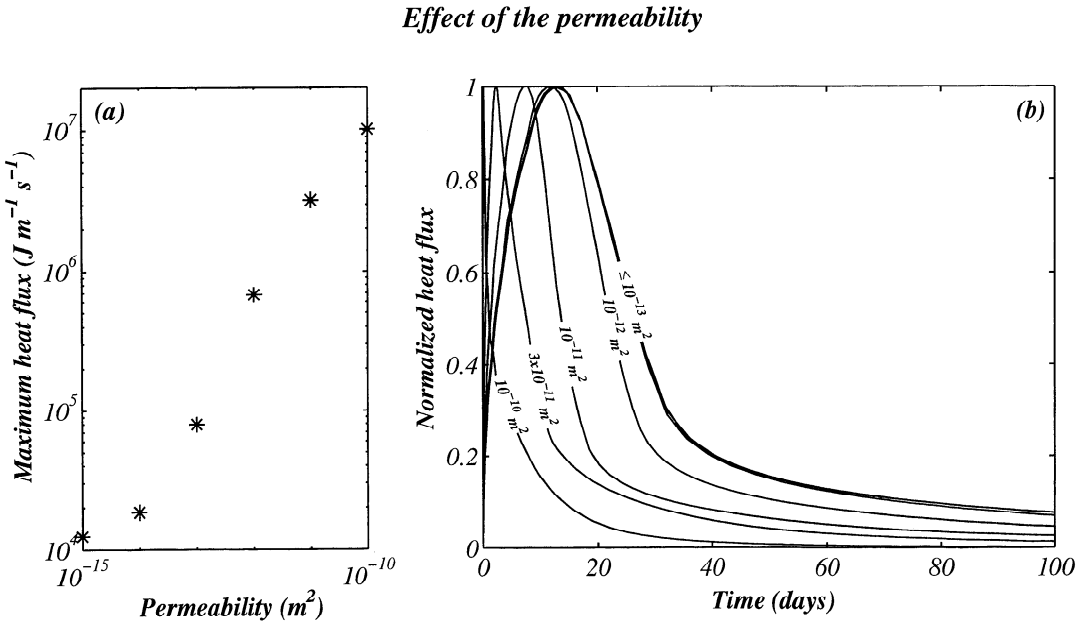

Figure 8. Surficial heat fluxes obtained from simulations of the cooling of a 2-m-wide dike intruded into a 500-m-thick porous layer saturated with cold fluid. The permeabilities are in the range 10^{-10}-10^{-15} m^2. (a) Maximum thermal fluxes are plotted versus permeability. (b) The temporal evolution of the surficial heat fluxes are shown normalized to the maxima of Figure 8a.

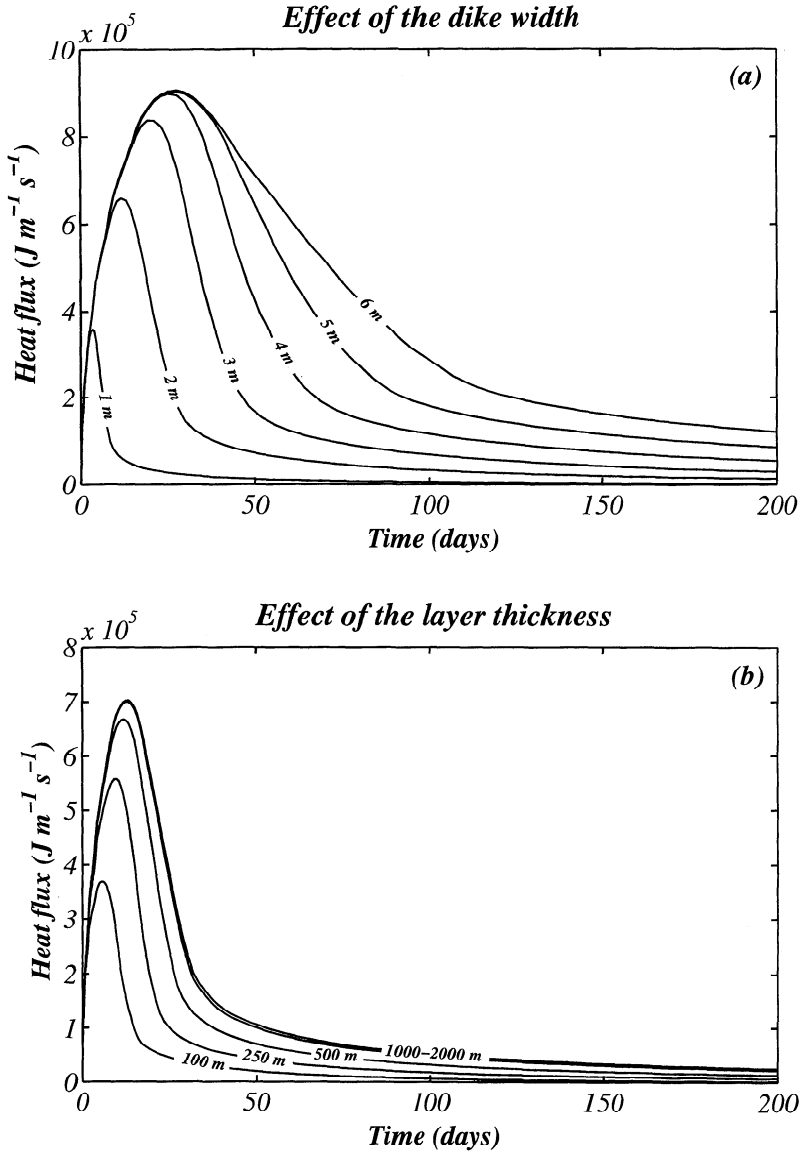

Figure 9. (a) Effects of the dike width on the surficial heat fluxes for a layer thickness of 500 m. (b) Effects of the layer thickness for a dike width of 2 m. In Figures 9a and 9b the permeability is 10^{-12} m^2.

crease in the decay times with dike width and layer thickness is a consequence of the increase in the total volume and heat content of the dike.

6. Fit to the Heat Flux Estimates

The heat fluxes estimated from the rise heights of the chronic plumes decrease to 20% of their maximum value in about 50 days at the flow site and about 90 days at the floc site. We chose to characterize the decay time as the time necessary for the heat fluxes to reach 20% of their maximum value because this is the largest decrease that is well constrained by the data (Figure 4). At both sites the maximum heat flux is $\sim 10^7$ J m^{-1} s^{-1}, but these estimates have large uncertainties. We obtained heat flux solutions for a wide range of dike widths, layer thicknesses, and permeabilities. We determined the characteristic decay times and the ratios Φ of the maximum observed to the maximum calculated heat fluxes and show contours of the results for h = 500 and 2000 m, w = 1-6 m, and k = 10^{-10}-10^{-15} m^2 in Figure 10. The stippled areas show the ranges of parameters that fit the data assuming the absolute heat flux estimates have an uncertainty of an order of magnitude. It is clear that the solution is nonunique. The decay of the heat fluxes observed in the chronic plumes of the CoAxial segment can be matched with permeabilities greater than $\sim 10^{-12}$ m^2, a dike width greater than about 2 m, and any layer thickness in the range 500-2000 m. However, for dikes less than 2 m wide the calculated decay times are too short. For permeabilities above 10^{-11} m^2 the decay times are also too short unless the dike is thicker than about 4 m at the flow site and about 6 m at the floc site. For permeabilities below $\sim 10^{-12}$ m^2 the observed decay times can be matched, but the absolute values of the heat fluxes are too low. Direct comparisons of the heat flux curves with the data show that the best fit to the trend of the estimated heat fluxes at the flow site is obtained with a 4-m-wide dike, a permeability of 10^{-11} m^2, and a layer thickness of 500 m (Figure 11a). The decay time at the floc site can be reproduced by decreasing the permeability, increasing the layer thick-

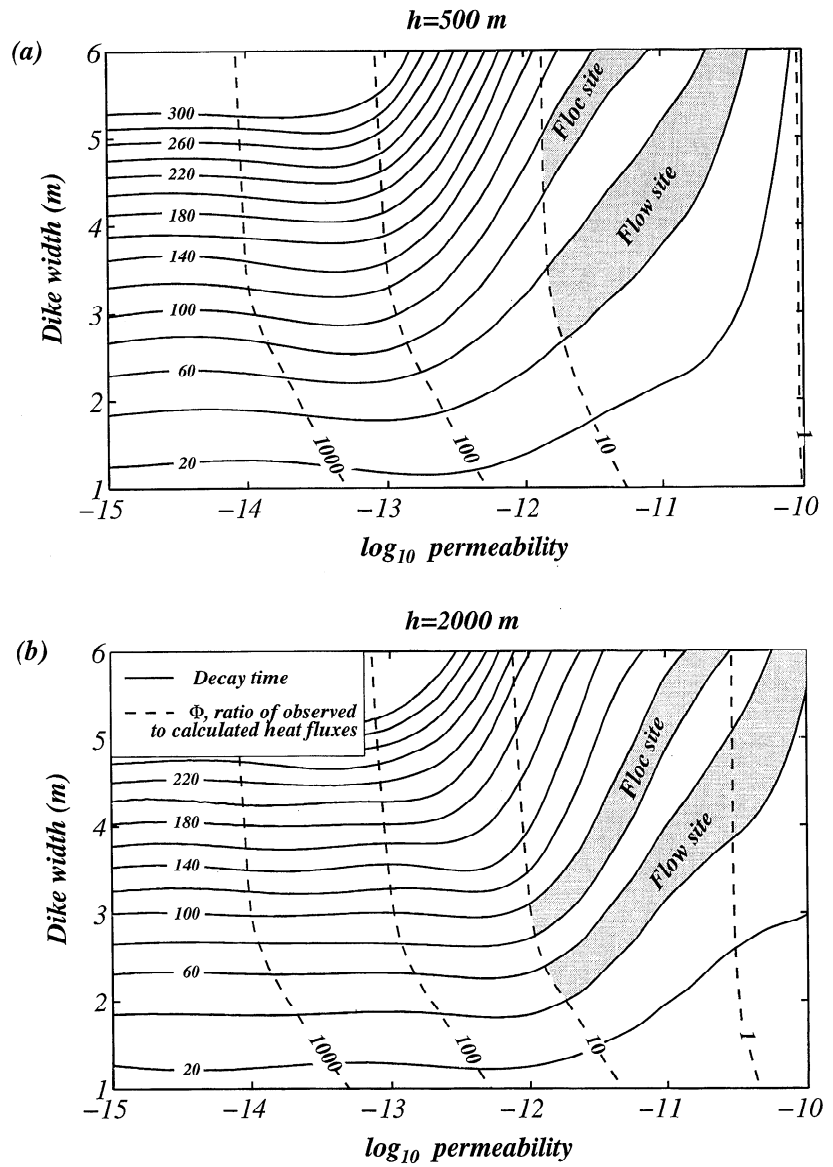

Figure 10. Compilation of the results from simulations of the convective cooling of the dike for a layer thickness of (a) h = 500 m and (b) h = 2000 m. The permeability and the dike width range from $k = 10^{-10}$-10^{-15} m^2 and w = 1-6 m, respectively. The solid lines are contours (20-day intervals) of the time required for the heat fluxes to decrease to 20% of their maximum value. The dashed lines are contours of Φ, the ratio of the maximum estimated to calculated heat fluxes. Because of the difficulties associated with determining absolute heat fluxes from plume rise heights, the estimated heat fluxes are assumed to be accurate to only an order of magnitude. The stippled areas delimit range of parameters which match the observations. A dike narrower than about 2 m wide cools too quickly, and permeabilities below ~10^{-12} m^2 yield heat fluxes that are too low.

ness, or increasing the dike width. The best fit is obtained by increasing the dike width to 5 m (Figure 11b).

7. Discussion

In the preceding section we have shown that the decay of the hydrothermal heat fluxes following the CoAxial diking event can be modeled by the injection of a thin dike into the upper oceanic crust. Although our simple model of this complex process yields good fit to the data, it is important to realize that our model has a number of significant limitations and our preferred solutions are certainly not unique. Before discussing the geological implications of our work we first discuss the assumptions underlying our model.

7.1. Model Assumptions

A key assumption of our model is that the porous medium can be represented by a continuum. This assumption is justified provided the scale of the flow is substantially larger than the mean crack spacing. Observations in ophiolites [*Nehlig*, 1994; *van Everdingen*, 1995] suggest that at depth, hydrothermal circulation occurs primarily through mesoscopic cracks with apertures of ~0.1-1 mm that are typically spaced 1-5 m apart. In shallow, unconsolidated pillow lavas the spacing of cracks is probably ~1 m, the diameter of individual pillows. In our solutions, upflow is confined to a narrow region extending only a few meters from the dike. Although crack densities may be high near the dike because of fracturing of the host rock during dike emplacement [*Pollard*, 1987; *Rubin*,

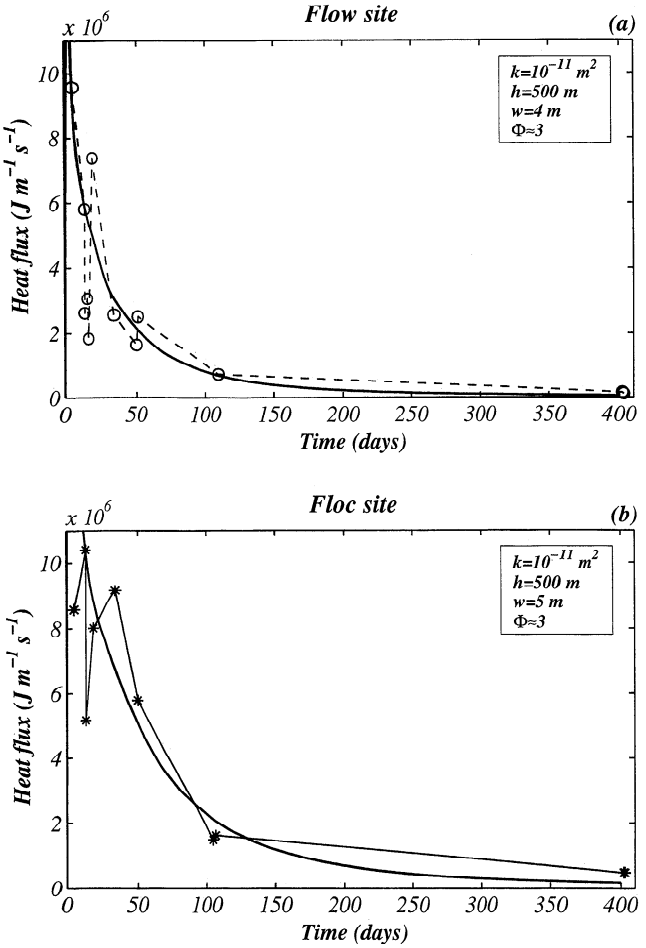

Figure 11. Best fits (thick solid lines) to the heat fluxes estimated for (a) the flow site and (b) the floc site. At the flow site the data (open circles, dashed line) are best modeled with $k = 10^{-11}$ m2, $h = 500$ m and $w = 4$ m. At the floc site the data (asterisks, thin solid line) are best fit with $k = 10^{-11}$ m^2, $h = 500$ m, and $w = 5$ m. Φ is the ratio of the maximum observed to the maximum calculated heat fluxes.

1993; *Lowell and Germanovich,* 1995; *Germanovich and Lowell,* 1995], it is not clear that our continuum assumption holds. If upflow occurs predominantly through microscopic cracks, then our model may significantly underestimate the large-scale permeability. Alternatively, if upflow occurs in mesoscopic fractures, variations in the configuration of fractures near the dike are likely to produce large local fluctuations in the characteristics of dike cooling. The advection of heat may be significantly retarded by the finite separation between the dike walls and the nearest mesoscopic fractures. Nevertheless, the maximum permeabilities estimated from the ophiolite observations of *Nehlig* [1994] and *van Everdingen* [1995] are in the same range as those used in simulations that yielded a good fit to the decay times of the heat fluxes.

Darcy's law assumes that flow within the cracks is laminar. The transition from laminar to turbulent flow occurs for Reynolds numbers in the range 10-100 [*Bear,* 1972]. The highest Darcy velocities obtained in our preferred models with $k = 10^{-12}$-10^{-11} m^2 are of the order of 10^{-4}-10^{-3} m s^{-1}. On the basis of a typical crack spacing of 1 m [*Nehlig,* 1994; *van Everdingen,* 1995] the maximum Reynolds number is ~10^3-10^4 which is clearly in the turbulent regime. However, even for these high permeabilities, most of the upflow and all the downflow falls in the laminar regime. It would be difficult to include turbulent flow in our model without better constraints on the characteristics of cracks adjacent to the dike.

We also assume that the dike was emplaced in a cold layer and that the base of the porous layer is adiabatic. Water column surveys of the area prior to the eruption showed no sign of hydrothermal discharge [*Baker et al.,* 1997]. The dike was apparently emplaced in a region where the combination of the geothermal gradient and the permeability was low enough to inhibit significant hydrothermal circulation. Convection appears in an open-top, horizontal, homogeneous, isotropic porous layer when the Rayleigh number

$$Ra = \frac{k\alpha_f \rho_f^2 c_{pf} g h \Delta T}{\mu_f \lambda_m} \qquad (11)$$

exceeds the critical value $Ra_c \sim 27.3$ [*Nield,* 1968], where ΔT is the temperature difference across the porous layer and the subscript f denotes fluid properties. Seismic observations on the CoAxial segment reveal an average layer 2A thickness of ~400 m [*Sohn et al.,* 1997]. Taking $\alpha_f = 10^{-4}$ °K^{-1}, $\rho_f = 1035$ kg m^{-3}, $c_{pf} = 4200$ J °K^{-1} kg^{-1}, $g = 10$ m s^{-2}, $\mu_f = 1.4 \times 10^{-3}$ Pa s and $\lambda_m = 2$ W m^{-1} °K^{-1} yields $\Delta T_c \sim 4 \times 10^{-11} \times k^{-1}$. However, this result is not very accurate when ΔT_c exceeds ~20°C because variations in fluid viscosity with temperature are significant. To investigate the effect of a geothermal gradient, we first determined numerically the onset of convection in a 400-m-thick layer with temperature-dependent fluid properties as defined in the model section. ΔT_c varied from 0.4°C for $k = 10^{-10}$ m^2 to 330°C for $k = 10^{-15}$ m^2. We then ran simulations with an initial temperature gradient corresponding to the calculated values of ΔT_c and a basal heat flux consistent with the initial thermal gradient. The resulting seafloor heat fluxes differed by less than 3% from those obtained with a uniformly cold layer. However, we cannot discount the possibility that low-level convective patterns, established before the dike was intruded, significantly affected its cooling.

Thermal contraction of the cooling dike is likely to generate permeability within the dike itself, facilitating heat extraction. For silicic rocks the brittle-plastic transition can occur at temperatures in the range 370-400°C [*Fournier,* 1991]; *Lister* [1974, 1983] suggests that basaltic rocks crack near 500°C. We ran simulations where the dike becomes permeable below a predefined threshold temperature (Figure 12). The sudden creation of permeability within the dike generates a burst in the heat fluxes, the amplitude and timing of which depend upon the cracking temperature. For high cracking temperatures the maximum heat flux increases significantly. Because of the uncertainties and timing of our heat flux estimates, we cannot determine whether cracking significantly affected the cooling of the CoAxial dike. However, the times for the heat flux to decay to 20% of its maximum value are not very sensitive to this process (Figure 12, inset). In these simulations we assigned the dike the same permeability as the host rock. If the permeability generated in the dike was higher, cooling would be faster since the flow is discharge controlled.

The permeability near the dike may change with time in response to chemical precipitation and thermal expansion. Assuming crack widths of the order of a millimeter, *Lowell and Germanovich* [1995] estimate that silica precipitation will take at least ~5 years to seal the permeability near the dike. *Wells and Ghiorso* [1991] suggest several decades are necessary for quartz precipitation to induce a substantial decrease in

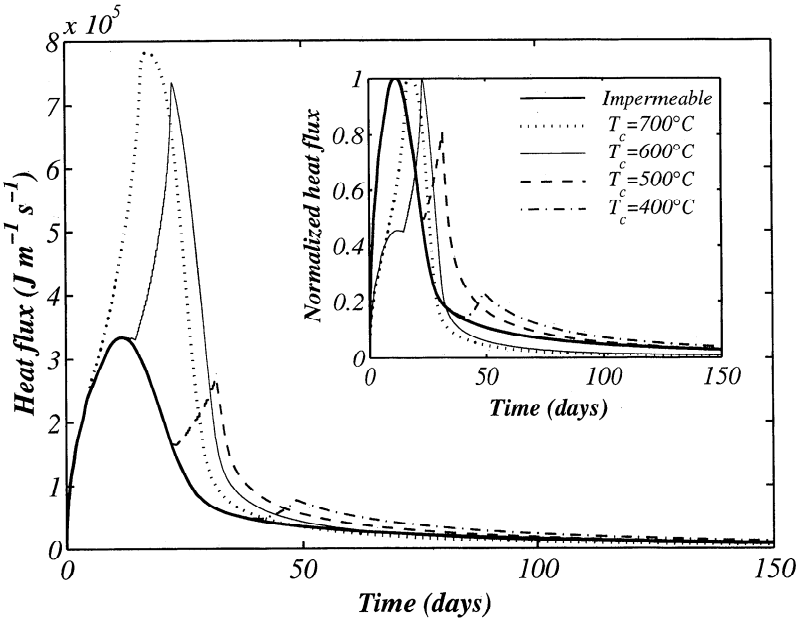

Figure 12. Heat fluxes calculated from simulations in which the dike becomes permeable when it cools below a threshold temperature. The dike is 2 m wide, the permeability in the host rock and permeable portions of the dike is 10^{-12} m^2, and the layer is 500 m thick. The cracking temperatures range from 400 to 700°C. The thick solid line shows the heat fluxes obtained with an impermeable dike. Note that all five curves are identical until cracking begins. Deviations from the solution for an impermeable dike occur when the boundary of the dike cools below the cracking temperature. Cracking produces a burst in the heat fluxes, which for higher cracking temperatures increases the maximum heat fluxes. The inset figure shows the heat fluxes normalized to the peak value for each simulation. The times for heat fluxes to decay to 20% of their maximum value are not affected significantly by cracking.

the porosity of oceanic hydrothermal systems. This process is unlikely to be significant over the timescales of our model. In contrast, thermoelastic sealing operates quickly, especially for finely spaced fractures [*Lowell,* 1990; *Germanovich and Lowell,* 1992; *Lowell et al.,* 1993] and may be an important process limiting the rate of heat advection.

We assume a homogeneous permeability, while borehole data suggests the permeability of the oceanic crust is strongly heterogeneous and irregularly distributed [*Anderson et al.,* 1985; *Becker,* 1996]. In particular, the permeability decreases with depth by several orders of magnitude in the upper crust. We have run several models which show that the presence of a low-permeability layer ($k < 10^{-13}$ m^2) underlying our model layer has little effect on the observed patterns of the heat fluxes. There is no doubt that our observations could be fit equally well with models in which the permeability decreases with depth.

Seismic data from the Juan de Fuca Ridge [*McDonald et al.,* 1994; *Sohn et al.,* 1997] suggest that the orientation of cracks is strongly anisotropic. Noting the elongated shape of vent fields on the Endeavour segment of the Juan de Fuca Ridge, *Wilcock and McNabb* [1996] argue that across-axis permeability may be an order of magnitude lower than in the orthogonal directions. *Ni and Beckermann* [1991] have addressed the problem of convection in a strongly anisotropic porous layer heated from the side. They show that high permeabilities in the vertical direction intensify the flow velocities and narrow the upflow zone near the heated wall. Since our model is discharge dominated and the upflow is vertical, our isotropic permeability would correspond to the vertical permeability of an anisotropic oceanic crust.

7.2. Geologic Implications

To reproduce the decay of our heat flux estimates for a dike intruded into a permeable layer of thickness in the range 500-2000 m, our model requires that the dike width and the permeability be greater than ~2 m and ~10^{-12} m^2, respectively. Such high permeabilities are consistent with measurements in highly permeable extrusives [*Anderson and Zoback,* 1982; *Becker,* 1996], and it is not unreasonable to infer that the observed seafloor heat fluxes arise from convective cooling within the extrusive layer. However, we cannot exclude the possibility that heat is extracted efficiently at greater depths. Investigations of black smoker systems [*Lowell and Burnell,* 1991; *Lowell and Germanovich,* 1994; *Wilcock and McNabb,* 1996] suggest that average bulk permeabilities of the order of 10^{-11}-10^{-13} m^2 may extend to depths of at least 1-2 km. High permeabilities may result also from fracturing of the rock in a narrow zone during the dike emplacement [*Pollard,* 1987; *Rubin,* 1993; *Lowell and Germanovich,* 1995; *Germanovich and Lowell,* 1995]. Convective flow would then be confined to a thin vertical channel adjacent to the dike. We performed simulations in which the porous layer has an aspect ratio $L/h \ll 1$. Because upflow is confined to a very narrow zone adjacent to the dike (Figure 6), such models yield heat flux decay times that differ by less than about 5% from the models with $L/h = 1$, provided the width of the highly permeable zone is at least 20 m.

The dike widths of 3-4 m obtained with our model are considerably larger than the commonly accepted value of 1 m determined from observations in ophiolites [e.g., *Kidd,* 1977]. *Tivey and Johnson* [1995] show that a magnetic profile across

the new lava flow is best modeled with a 10-m-wide nonmagnetic intrusion, although they do not equate this region to a single dike. It is conceivable that ophiolitic models may not apply to CoAxial because it is not a typical segment of oceanic crust because of the presence of Axial volcano to the south. However, it is more likely that we overestimate the dike widths because of the limitations of the continuum assumption discussed above. Because the decay time in a permeable layer is controlled by the conductive length scale, the decay of heat fluxes for a 1-m-wide dike which is separated by ~1 m from the nearest cracks on either side is probably similar to that for a 3-m-wide dike in a permeable continuum.

The size and height of the CoAxial event plumes require that they were formed by the release of 2-10 x 10^{15} J of hydrothermal heat [*Baker et al.*, 1995a] in a matter of hours [*Lavelle*, 1995]. Several mechanisms have been proposed to explain the formation of event plumes from fluids circulating deep within the crust [*Cann and Strens*, 1989; *Cathles*, 1993; *Lowell and Germanovich*, 1995; *Wilcock*, 1997]. All the mechanisms advanced require permeabilities in the range 10^{-9}-10^{-10} m^2 to support the extremely high discharge rates necessary to form event plumes. *Lowell and Germanovich* [1995] propose that event plumes form by the cooling of the dike. In constructing our model we have tacitly assumed that this is not the case. If the plumes did form from the cooling of a shallow intrusion in an extremely permeable layer, then our model layer would represent the region underlying this superficial layer. *Butterfield et al.* [1997] propose a model in which the formation of the CoAxial event plumes results primarily from the cooling of the lava erupted on the seafloor. They argue that this model accounts for the coincidence of the event plumes and the eruption, the size and the formation times of event plumes, and the presence of halite coatings and high-temperature sulfides on the fresh extrusives. This model seems most consistent with our study.

The estimated heat fluxes of the chronic plumes at the flow site decayed about 2 times faster than at the floc site (Figure 4). This difference is also apparent in the temporal evolution of the bacterial activity and the chemistry of the chronic plumes fluids. For instance, no thermophile bacteria could be isolated from venting fluids at the flow site in October 1993, while they were present at the floc site at that time [*Holden*, 1996]. Chemically, the fluids are Fe-rich at the flow site and more reducing, H_2S-rich at the floc site [*Butterfield et al.*, 1997]. These observations suggest that there was a longer-lasting interaction between the dike and the circulating fluids at the floc site. *Butterfield et al.* [1997] argue that the heat source is deeper at the floc site. This explanation is consistent with our model although the differences between the heat fluxes at the floc and the flow sites can also be modeled by changing the permeability or the dike width.

While venting had stopped almost completely at the flow site 1 year after the eruption [*Embley et al.*, 1994; *Butterfield et al.*, 1997], remnant heat fluxes were still measurable at the floc site after 2 years [*Butterfield et al.*, 1997]. Our model of the convective cooling of a dike does not reproduce these remnant heat fluxes very well. One possible explanation is that the remnant heat fluxes result from convective cooling within a lower-permeability layer underlying the extrusives. Another explanation is that fracturing during the dike injection opened up new hydrothermal pathways to a region of hot rock beneath the floc site. The presence of such a heat source beneath the floc site is not unreasonable since this site is close to the north rift zone of Axial volcano, the inferred source of the magma [*Dziak et al.*, 1995; *Embley et al.*, 1995].

In our model the dike extends to the seafloor. However, there was no eruption at the floc site, and we have investigated a model where the dike stops at a depth d below the surface. Figure 13 shows the resulting heat fluxes at the seafloor for several values of d, for a 1-m-wide dike, a permeability of 10^{-12} m^2, and a layer thickness d + 500 m. Even when the dike shallows to within ~25 m beneath the seafloor, the maximum heat fluxes at the surface are considerably decreased and are delayed by tens of days. Our Darcy continuum model probably overestimates this effect because near-surface fissures must provide an efficient means to tap heat from a buried dike. Faulting

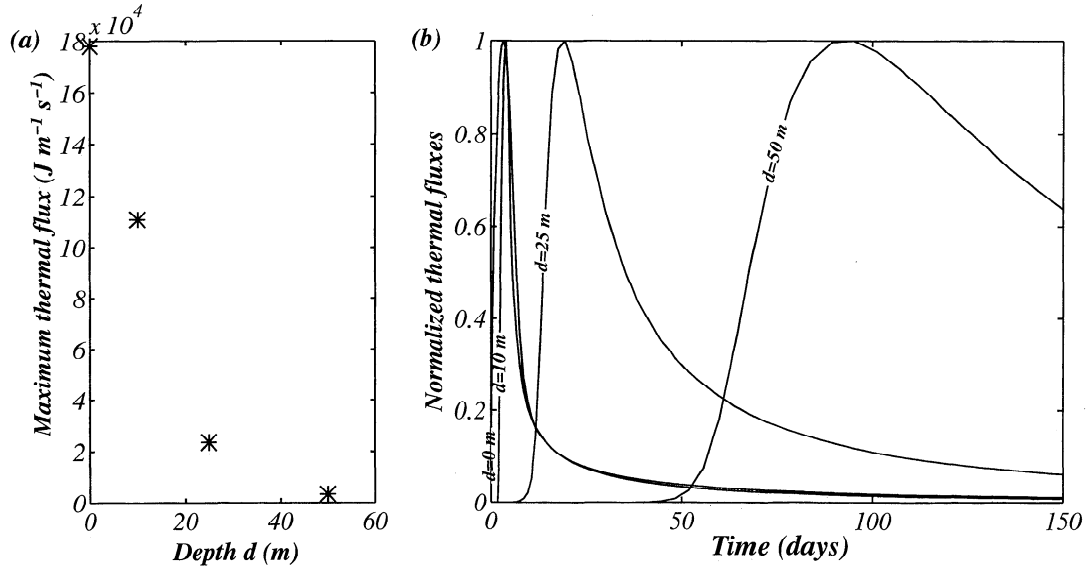

Figure 13. Heat fluxes calculated from simulations in which the top of the dike is at a depth d below the seafloor. Heat fluxes for d = 0, 10, 25 and 50 m are shown for a 1-m-wide dike, a permeability of 10^{-12} m^2, and a layer thickness d + 500 m. (a) Maximum heat fluxes are shown as a function of the depth. (b) Heat fluxes normalized to the maximum value shown in Figure 13a are plotted against time.

above the propagating dike [*Pollard,* 1987; *Rubin,* 1993] may also open up fluid pathways to the surface. Nevertheless, this result suggests that the top of the dike may be fairly shallow at the floc site.

The water column observations of July 1993 [*Embley et al.,* 1995] show that initially, the chronic plumes extended almost continuously between the flow and floc sites (Figure 2). Whether the venting itself was initially continuous is not known because near-bottom observations were limited to the floc and flow sites. It does appear from the water column observations (Figure 2) that venting was more intense at these two sites. We hypothesize that the flow and the floc sites are regions where the dike penetrated the layer of highly permeable extrusives, thus gaining access to permeable pathways to the seafloor. Between the floc and the flow sites, either the top of the dike is deeper or the extrusive layer thinner. Qualitatively, three-dimensional flow is likely to increase the decay times and the absolute value of heat fluxes.

8. Conclusions

We have investigated the convective cooling of a dike intruded into a fluid-saturated porous layer of uniform permeability. The interplay between horizontal conduction across the dike wall and vertical advection within the porous layer controls the transfer of heat to the seafloor, and the temporal evolution of the surficial heat fluxes is affected by the permeability, layer thickness, and dike width. Although certainly not a unique solution, our model can reproduce the temporal evolution of the heat fluxes estimated from the rise heights of the chronic plumes. For a dike height in the range 500-2000 m, these heat fluxes constrain the permeability to be higher than $\sim 10^{-12}$ m^2 and the dike width to be greater than about 2 m. If the dike width is assumed to be less than about 5 m, then the permeability is constrained to the range 10^{-11}-10^{-12} m^2. These high permeabilities are consistent with flow through highly permeable extrusives or with the creation of a high permeability zone due to fracturing during the dike emplacement. However, they are about 2 orders of magnitude less than the permeabilities required to explain the formation of event plumes from fluids deep within the crust.

This study shows that a time series of hydrothermal plume observations can place strong constraints on the cooling of subseafloor magmatic intrusions. Early observations are essential because decay of the convective heat fluxes can occur very quickly. Although it is very difficult to determine accurately the heat input into deep-sea plumes, this study demonstrates the importance of obtaining good estimates of the absolute value of the heat fluxes as well as their relative values.

Acknowledgments. We would like to thank John Delaney and the Volcano System Center (VSC) at the University of Washington for supporting our modeling efforts by making available a DEC Alpha 3000/600 on which all computations were performed. We acknowledge Russell McDuff, David Butterfield and Mitsuhiro Kawase for useful comments during the preparation of this manuscript and Margaret Tivey, Robert Lowell and Andrew Fisher for thorough reviews. This study was supported by a Fulbright Fellowship award to A. S. M. Cherkaoui, the NOAA VENTS program, and the National Science Foundation under grant OCE-9629425. Contribution 1789 from NOAA/Pacific Marine Environmental Laboratory.

References

Anderko, A., and K. S. Pitzer, Equation-of-state representation of phase equilibria and volumetric properties of the system NaCl-H_2O above 573 K, *Geochim. Cosmochim. Acta, 57,* 1657-1680, 1993.

Anderson, R. N., and M. D. Zoback, Permeability, underpressures, and convection in the oceanic crust near the Costa Rica Rift, eastern equatorial Pacific, *J. Geophys. Res., 87,* 2860-2868, 1982.

Anderson, R. N., M. D. Zoback, S. H. Hickam, and R. L. Newmark, Permeability versus depth in the upper oceanic crust, in situ measurements in Deep Sea Drilling Project hole 504B, eastern equatorial Pacific, *J. Geophys. Res., 90,* 3659-3669, 1985.

Baker, E. T., G. J. Massoth, and R. A. Feely, Cataclysmic hydrothermal venting on the Juan de Fuca Ridge, *Nature, 329,* 149-151, 1987.

Baker, E. T., J. W. Lavelle, R. A. Feely, G. J. Massoth, S. L. Walker, and J. E. Lupton, Episodic venting of hydrothermal fluids from the Juan de Fuca Ridge, *J. Geophys. Res., 94,* 9237-9250, 1989.

Baker, E. T., G. J. Massoth, G. A. Cannon, R. A. Feely, J. E. Lupton, R. E. Thomson, J. F. Gendron, B. J. Burd, and R. W. Embley, Temporal and spatial patterns of chronic and event hydrothermal plumes at the CoAxial vent field, Juan de Fuca Ridge, July 1 to October 20, 1993 (abstract), *Eos Trans. AGU, 74*(43), Fall Meet. Suppl., 619, 1993.

Baker, E. T., G. T. Massoth, R. A. Feely, R. W. Embley, R. E. Thomson, and B. J. Burd, Hydrothermal event plumes from the CoAxial seafloor eruption site, Juan de Fuca Ridge, *Geophys. Res. Lett., 22,* 147-150, 1995a.

Baker, E. T., C. R. German, and H. Elderfield, Hydrothermal plumes over spreading-center axes: Global distributions and geological inferences, in *Seafloor Hydrothermal Systems: Physical, Chemical, Biological, and Geological Interactions, Geophys. Monogr. Ser.,* vol. 91, edited by S. E. Humphris et al., pp. 317-346, AGU, Washington, D. C., 1995b.

Baker, E. T., G. J. Cannon, J. E. Lupton, S. L. Walker, D. A. Tennant, C. Wilson, and N. Garfield, Time-series sampling of hydrothermal event plume(s) from the 1996 Gorda Ridge eruption (abstract), *Eos Trans. AGU, 77*(46), Fall Meet. Suppl., F1, 1996.

Baker, E. T., G. J. Massoth, R. A. Feely, G. A. Cannon, and R. E. Thomson, The rise and fall of the CoAxial hydrothermal site, 1993-1996, *J. Geophys. Res.,* in press, 1997.

Bear, J., *Dynamics of Fluids in Porous Media,* Elsevier, New York, 1972.

Becker, K., Permeability measurements in hole 896A and implications for the lateral variability of upper crustal permeability at sites 504 and 896, edited by J. C. Alt et al., *Proc. Ocean Drill. Program Sci. Results, 148,* 353-363, 1996.

Briggs, G. A., *Plume Rise,* U.S. At. Energy Comm., Washington, D. C., 1969.

Brikowski, T., and D. Norton, Influence of magma chamber geometry on hydrothermal activity at mid-ocean ridges, *Earth Planet. Sci. Lett., 93,* 241-255, 1989.

Butterfield, D. A., I. R. Jonasson, G. J. Massoth, R. A. Feely, K. K. Roe, R. E. Embley, J. F. Holden, R. E. McDuff, M. D. Lilley, and J. R. Delaney, Seafloor eruptions and evolution of hydrothermal fluid chemistry, *Philos. Trans. R. Soc. London. A., 355,* 369-386, 1997.

Cann, J. R., and M. R. Strens, Modeling periodic megaplume emission by black smoker systems, *J. Geophys. Res., 94,* 12,227-12,237, 1989.

Cannon, G. A., D. J. Pashinski, and T. J. Stanley, Fate of hydrothermal plumes on the Juan de Fuca Ridge, *Geophys. Res. Lett., 22,* 163-166, 1995.

Cathles, L. M., A capless 350°C flow zone model to explain, megaplumes, salinity variations, and high-temperature veins in ridge axis hydrothermal systems, *Econ. Geol., 88,* 1977-1988, 1993.

Chadwick, W. W., Jr., and R. W. Embley, Lava flows from a mid-1980s submarine eruption on the Cleft segment, Juan de Fuca Ridge, *J. Geophys. Res., 99,* 4761-4776, 1994.

Chadwick, W. W., Jr., R. W. Embley, and C. G. Fox, Evidence for volcanic eruption on the southern Juan de Fuca Ridge between 1981 and 1987, *Nature, 350,* 416-418, 1991.

Cheng, P., and W. J. Minkowycz, Free convection about a vertical flat plate embedded in a porous medium with application to heat transfer from a dike, *J. Geophys. Res., 82,* 2040-2044, 1977.

Cheng, P., and I. Pop, Transient free convection about a vertical flat plate embedded in a porous medium, *Int. J. Eng. Sci., 22,* 253-264, 1984.

Crisp, J., Rates of magma emplacement and volcanic output, *J. Volcanol. Geotherm. Res., 20,* 177-211, 1984.

Delaney, P. T., Heat transfer during emplacement and cooling of mafic dykes, in *Mafic Dyke Swarms,* edited by H. C. Falls and W. F. Fahrig, *Geol. Assoc. Can. Spec. Pap., 34,* 31-46, 1987.

Delaney, J. R., and R. W. Embley, An October response cruise to the June-July intrusive/eruptive events at the CoAxial segment of the Juan de Fuca Ridge (abstract), *Eos Trans. AGU, 74*(43), Fall Meet. Suppl., 620, 1993.

Dziak, R. P., C. G. Fox, and A. E. Schreiner, The June-July 1993 seismoacoustic event at CoAxial segment, Juan de Fuca Ridge: Evidence for a lateral dike injection, *Geophys. Res. Lett.*, *22*, 135-138, 1995.

Embley, R. W., and W. W. Chadwick Jr., Volcanic and hydrothermal processes associated with a recent phase of seafloor spreading at the northern Cleft segment: Juan de Fuca Ridge, *J. Geophys. Res.*, *99*, 4741-4760, 1994.

Embley, R. W., W. W. Chadwick, M. R. Perfit, and E. T. Baker, Geology of the northern Cleft segment, Juan de Fuca Ridge: Recent lava flows, sea-floor spreading, and the formation of megaplumes, *Geology*, *19*, 771-775, 1991.

Embley, R. W., et al., Comparison of two recent eruptive sites on the Juan de Fuca ridge: Geological setting and time-series observations (abstract), *Eos Trans. AGU*, *75*(44), Fall Meet. Suppl., 617, 1994.

Embley, R. W., W. W. Chadwick Jr., I. R. Jonasson, D. A. Butterfield, and E. T. Baker, Initial results of the rapid response to the 1993 CoAxial event: Relationships between hydrothermal and volcanic processes, *Geophys. Res. Lett.*, *22*, 143-146, 1995.

Fournier, R. O., The transition from hydrostatic to greater than hydrostatic fluid pressure in presently active continental hydrothermal systems in crystalline rock, *Geophys. Res. Lett.*, *18*, 955-958, 1991.

Fox, C. G., Special collection on the June 1993 volcanic eruption on the CoAxial segment, Juan de Fuca Ridge, *Geophys. Res. Lett.*, *22*, 129-130, 1995.

Fox, C. G., W. E. Radford, R. P. Dziak, T-K. Lau, H. Matsumoto, and A. E. Schreiner, Acoustic detection of a seafloor spreading episode on the Juan de Fuca Ridge using military hydrophone arrays, *Geophys. Res. Lett.*, *22*, 131-134, 1995.

Francheteau, J., R. Armijo, J. L. Cheminée, R. Hekinian, P. Lonsdale, and N. Blum, Dyke complex of the East Pacific Rise exposed in the walls of Hess Deep and the structure of the upper oceanic crust, *Earth Planet. Sci. Lett.*, *111*, 109-121, 1992.

Gartling, D. K., and C. E. Hickox, A numerical study of the applicability of the Boussinesq approximation for a fluid-saturated porous medium, *Int. J. Numer. Methods Fluids*, *5*, 995-1013, 1985.

Germanovich, L. N., and R. P. Lowell, Percolation theory, thermoelasticity, and discrete hydrothermal venting in the Earth's crust, *Science*, *255*, 1564-1567, 1992.

Germanovich, L. N., and R. P. Lowell, The mechanism of phreatic eruptions, *J. Geophys. Res.*, *100*, 8417-8434, 1995.

Grigull, U., *Steam Tables in SI units*, edited by U. Grigull, J. Straub, and P. Schiebener, p. 53, Springer-Verlag, New York, 1984.

Haymon, R. M., et al., Volcanic eruption of the mid-ocean ridge along the East Pacific Rise crest at 9°45-52'N: Direct submersible observations of seafloor phenomena associated with an eruption event in April, 1991, *Earth Planet. Sci. Lett.*, *119*, 85-101, 1993.

Holden, J. F., Ecology, diversity, and temperature-pressure adaptation of the deep-sea hyperthermophilic archaea Thermococcales, Ph.D. dissertation, Univ. of Washington, Seattle, 1996.

Juniper, S. K., P. Martineu, J. Sarrazin, and Y. Gélinas, Microbial-mineral floc associated with nascent hydrothermal activity on CoAxial segment, Juan de Fuca Ridge, *Geophys. Res. Lett.*, *22*, 179-182, 1995.

Kidd, R. G. W., A model for the formation of the upper oceanic crust, *Geophys. J. R. Astron. Soc.*, *50*, 149-183, 1977.

Lavelle, J. W., The initial rise of a hydrothermal plume from a line segment source: Results from a three-dimensional numerical model, *Geophys. Res. Lett.*, *22*, 159-162, 1995.

Lister, C. R. B., On the penetration of water into hot rocks, *Geophys. J. R. Astron. Soc.*, *39*, 465-509, 1974.

Lister, C. R. B., The basic physics of water penetration into hot rocks, in *Hydrothermal Processes at Seafloor Spreading Centers*, edited by P. A. Rona, et al., pp. 141-168, Plenum, New York, 1983.

Lowell, R. P., Thermoleasticity and the formation of black smokers, *Geophys. Res. Lett.*, *17*, 709-712, 1990.

Lowell, R. P., and D. K. Burnell, Mathematical modeling of conductive heat transfer from a freezing, convecting magma chamber to a single-pass hydrothermal system: Implications for seafloor black smokers, *Earth Planet. Sci. Lett.*, *104*, 59-69, 1991.

Lowell, R. P., and L. N. Germanovich, On the temporal evolution of high-temperature hydrothermal systems at ocean ridge crests, *J. Geophys. Res.*, *99*, 565-575, 1994.

Lowell, R. P., and L. N. Germanovich, Dike injection and the formation of megaplumes at ocean ridges, *Science*, *267*, 1804-1807, 1995.

Lowell, R. P., P. Van Cappellen, and L. N. Germanovich, Silica precipitation in fractures and the evolution of permeability in hydrothermal upflow zones, *Science*, *260*, 192-194, 1993.

Lupton, J. E., Hydrothermal plumes: Near and far field, in *Seafloor Hydrothermal Systems: Physical, Chemical, Biological, and Geological Interactions*, *Geophys. Monogr. Ser.*, vol. 91, edited by S. E. Humphris et al., AGU, Washington, D. C., pp. 317-346, 1995.

Macdonald, K. C., R. M. Haymon, and A. Shor, A 220 km^2 recently erupted lava field on the East Pacific Rise near latitude 8°S, *Geology*, *17*, 212-216, 1989.

McDonald, M. A., S. C. Webb, J. A. Hildebrand, B. D. Cornuelle, and C. G. Fox, Seismic structure and anisotropy of the Juan de Fuca Ridge at 45°N, *J. Geophys. Res.*, *99*, 4857-4873, 1994.

McDuff, R. E., Physical dynamics of deep-sea hydrothermal plumes, in *Seafloor Hydrothermal Systems: Physical, Chemical, Biological, and Geological Interactions*, Geophys. Monogr. Ser., vol. 91, edited by S. E. Humphris et al., pp. 357-368, AGU, Washington, D. C., 1995.

Middleton, J. M., and R. E. Thomson, Modelling the rise of hydrothermal plumes, *Can. Tech. Rep. Hydrogr. Ocean Sci. 69*, 18 pp., Can. Dep. of Fish. and Oceans, Sidney, B. C., Canada, 1986.

Morton, B. R., G. I. Taylor, and J. S. Turner, Turbulent gravitational convection from maintained and instantaneous sources, *Proc. R. Soc. London A*, *234*, 1-23, 1956.

Nehlig, P., Fracture and permeability analysis in magma-hydrothermal transition zones in the Samail ophiolite (Oman), *J. Geophys. Res.*, *99*, 589-601, 1994.

Ni, J., and C. Beckermann, Natural convection in a vertical enclosure filled with anisotropic porous media, *J. Heat Transfer*, *113*, 1033-1037, 1991.

Nield, D. A., Onset of thermohaline convection in a porous medium, *Water Resour. Res.*, *4*, 553-560, 1968.

Parmentier, E. M., Two phase natural convection adjacent to a vertical heated surface in a permeable medium, *Int. J. Heat Mass Transfer*, *22*, 849-855, 1979.

Patankar, S. V., *Numerical Heat Transfer and Fluid Flow*, 153 pp., Hemisphere, Washington, D. C., 1980.

Patterson, P. K., and R. P. Lowell, Numerical models of hydrothermal circulation for the intrusion zone at an ocean ridge axis, in *The Dynamic Environment of the Ocean Floor*, edited by K. A. Fanning and F. T. Manheim, pp. 471-492, Lexington Books, Lexington, Mass., 1982.

Pitzer, K. C., J. C. Peiper, and R. H. Busey, Thermodynamic properties of aqueous sodium chloride solutions, *J. Phys. Chem. Ref. Data*, *13*, 1-102, 1984.

Pollard, D. D., Elementary fracture mechanics applied to the structural interpretation of dykes, in *Mafic Dyke Swarms*, edited by H. C. Falls and W. F. Fahrig, *Geol. Assoc. Can. Spec. Pap.*, *34*, 5-24, 1987.

Pond, S., and G. L. Pickard, *Introductory Dynamic Oceanography*, 329 pp., Pergamon, Tarrytown, N. Y., 1983.

Renard, V., R. Hekinian, J. Francheteau, R. D. Ballard, and H. Backer, Submersible observations at the axis of the ultra-fast spreading East Pacific rise (17°30'S to 21°30'S), *Earth Planet. Sci. Lett.*, *75*, 339-353, 1985.

Rubin, A. M., Tensile fracture of rock at high confining pressure: Implications for dike propagation, *J. Geophys. Res.*, *98*, 15,919-15,935, 1993.

Shiralkar, G. S., M. Haajizadeh, and C. L. Tien, Numerical study of high Rayleigh number convection in a vertical porous enclosure, *Numer. Heat Transfer*, *6*, 223-234, 1983.

Sohn, R. A., S. C. Webb, J. A. Hildebrand, and B. D. Cornuelle, Three-dimensional tomographic velocity structure of the upper crust, CoAxial segment, Juan de Fuca Ridge: Implications for on-axis evolution and hydrothermal circulation, *J. Geophys. Res.*, *102*, 17,679-17,695, 1997.

Spiess, F. N., and J. A. Hildebrand, Deep tow studies of recent activity on the Juan de Fuca Ridge, (abstract), *Eos Trans. AGU*, *74*(43), Fall Meet. Suppl., 620, 1993.

Tivey, M. A., and H. P. Johnson, Alvin magnetic survey of zero-age crust: CoAxial segment eruption, Juan de Fuca Ridge 1993, *Geophys. Res. Lett.*, *22*, 171-174, 1995.

Touloukian, Y. S., W. R. Judd, and R. F. Roy (Eds.), *Physical Properties of Rocks and Minerals*, 548 pp., McGraw-Hill, New York, 1981.

Turcotte, D. L., and G. Shubert, *Geodynamics: Applications of Continuum Physics to Geological Problems*, 450 pp., John Wiley, New York, 1982.

Turner, J. S., *Buoyancy Effects in Fluids*, Cambridge Univ. Press, New York, 1973.

Turner, J. S., Turbulent entrainment: The development of the entrainment assumption and its application to geophysical flows, *J. Fluid Mech.*, *173*, 431-471, 1986.

van Everdingen, D. A., Fracture characteristics of the sheeted dike complex, Troodos ophiolite, Cyprus: Implications for permeability of oceanic crust, *J. Geophys. Res., 100*, 19,957-19,972, 1995.

Walker, K. L., and G. M. Homsy, Convection in a porous cavity, *J. Fluid Mech., 87*, 449-474, 1978.

Wells, J. T., and M. S. Ghiorso, Coupled fluid flow and reaction in mid-ocean ridge hydrothermal systems: The behavior of silica, *Geochim. Cosmochim. Acta, 55*, 2467-2481, 1991.

Wilcock, W. S. D., A model for the formation of transient event plumes above mid-ocean ridge hydrothermal systems, *J. Geophys. Res., 102*, 12,109-12,121, 1997.

Wilcock, W. S. D., and A. McNabb, Estimates of crustal permeability on the Endeavour segment of the Juan de Fuca mid-ocean ridge, *Earth Planet. Sci. Lett., 138*, 83-91, 1996.

Xu, W., and R. P. Lowell, Numerical modeling of two-phase seafloor hydrothermal systems caused by dike intrusion (abstract), *Eos Trans. AGU, 77*(46), Fall Meet. Suppl., 728, 1996.

Yusufova, V. D., R. I. Pepinov, V. A. Nicolayev, G. U. Zokhrabbekova, N. V. Lobcova, and T. D. Tuayev, Thermophysical properties of softened seawater and salt solutions over a wide temperature and pressure range, *Desalination, 25*, 269-280, 1978.

E. T. Baker, Pacific Marine Environmental Laboratory, NOAA Building 3, 7600 Sand Point Way NE, Seattle, WA 98115.

A. S. M. Cherkaoui and W. S. D. Wilcock, School of Oceanography, University of Washington, P. O. box 357940, Seattle, WA 98195. (e-mail: abdul@ocean.washington.edu; wilcock@ocean.washington.edu)

(Received November 8, 1996; revised June 17, 1997; accepted July 24, 1997.)